Proceedings of the 9th International Conference on Cyclotrons and their Applications
September 1981, Caen, France

DESIGN CALCULATIONS FOR THE CENTRAL REGION OF THE NSCL 500 MEV SUPERCONDUCTING CYCLOTRON*

F. Marti, M.M. Gordon, M.B. Chen,[a] C. Salgado, T. Antaya and E. Liukkonen[b]

Cyclotron Laboratory, Michigan State University, East Lansing, MI 48824 USA

Abstract.-The 500 MeV superconducting cyclotron has three 60° dees within the magnet valleys, and the design of the central region is complicated because it must accommodate the inner tips of these dees, the tips of the three intervening dummy dees, and the ion source, all within a very small space. In addition, this cyclotron is designed to operate on harmonics from h=1 to 7, with dee voltages up to 100 kV, and must accelerate a wide variety of heavy ions with turn numbers from n=100 to 600. To satisfy these diverse requirements, the overall plan for the central region calls for the construction and use of many different, but readily interchangeable sets of electrode structures with each set designed for a different range of operating conditions.

The procedure for determining the optimum geometry for a set of electrodes involves a converging sequence of tentative designs each of which is tested and improved through a combination of electrolytic tank measurements and orbit computations. For this purpose, the speed and accuracy of the tank measurements have been improved, and the resultant potentials are used in our computer programs to determine whether the ion orbits clear the obstacles successfully, gain energy efficiently, receive adequate vertical focusing, and finally emerge from the central region properly centered. The vertical motion computations are by far the most difficult, and a special effort has been made to obtain satisfactory results.

The 3D-Cyclone orbit program is an important tool for the design of the electrode structures in the central region of the 500 MeV superconducting cyclotron.[1] This program is a revised and enlarged version of the Cyclone code used in the design of our old 50 MeV cyclotron.[2] In addition to computing orbits in the electric field of a three dee rf system, the new program can also calculate the linear z motion in these fields.

The 3D-Cyclone program actually consists of three separate orbit codes which have been woven together so as to make possible the tracking of ion orbits starting from the source slit and going all the way out to the middle of the machine. Part I takes the ion from the source slit out to just beyond the puller. Part II continues the orbit for a few turns until it reaches r=2.8 in. Part III then takes the orbit as far as desired. These three parts differ mainly in the way they treat the rf electric field.

All three parts use the same median plane magnetic field $B(r,\theta)$ which is stored in a polar mesh with $\Delta\theta$=1.0 deg, and Δr=0.5 in. All such fields are produced by a separate set of special programs which tailor these fields to satisfy specific focusing and isochronism requirements. The magnetic field provides an absolute reference frame for positioning all of the electrodes and the resultant electric field used in the 3D-cyclone program.

For a given electrode geometry, an electrolytic tank is used to measure the median plane potentials $U(x,y)$ in a square mesh measuring 5.6 in on a side and with a uniform spacing $\Delta x = \Delta y$ = 40 mils. Each potential map thus contains 140 x 140 points and, because of recent improvements, now requires only 4 hours to measure. The accuracy and smoothness of the data have been tested using the geometry shown in fig. 1, and seem satisfactory for our purposes.

In Part I, the electric field in the source-puller region is derived from the potential: $V(x,y,t) = U_o(x,y)\sin\omega_{rf}t$, where $U_o(x,y)$ is mapped using an enlarged scale model of the electrode structures, and a sample map is shown in fig. 2. Such potential maps are

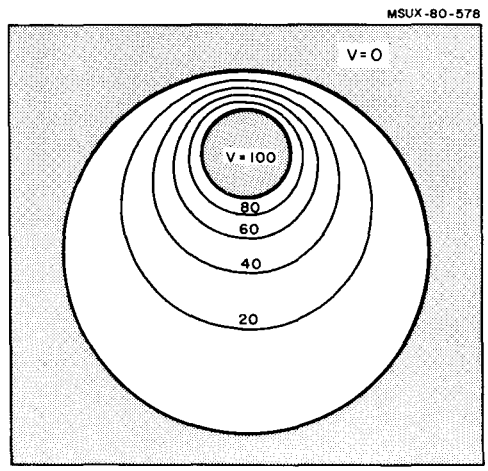

Fig. 1: Electrolytic tank test set-up. To check the accuracy of the electrolytic tank facility, we measured the potential between two cylinders. This is a two dimensional geometry where one of the cylinders is inside the other, but not coaxial with it. The theoretical potential distribution is given by a fairly simple analytic expression. The discrepancies between measurement and theory are within one percent of the potential difference applied between electrodes. This figure shows the equipotentials derived from such a measurement. The largest deviations occur when the probe is very close to the electrodes.

available for several different source-puller geometries, since each geometry will be fixed in the machine except for a possible rotation of the ion source by ±5 deg about its axis. The orbit computations in this part of the program are carried out in cartesian coordinates with t as the independent variable, and do not include z motion.

The electric field for Part II of the program is more complicated. The three dees with the three intervening dummy dees, along with the ion source, all

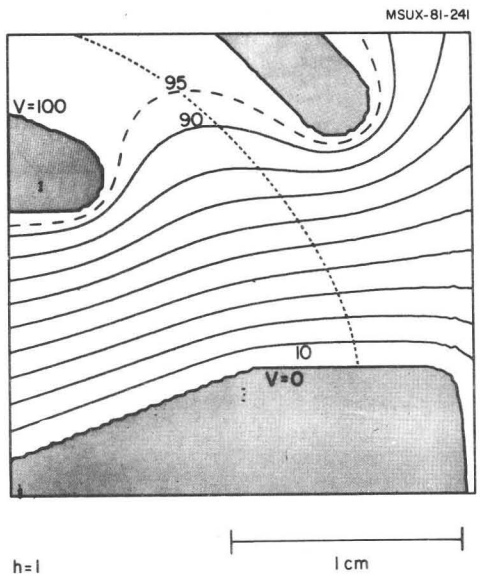

Fig. 2: Source-to-puller geometry for h=1. As described in the text, the 3D-Cyclone code calculates orbits of ions using the electric fields derived from measurements of the electric potential in the electrolytic tank. This figure shows the equipotentials obtained in the region between ion source and puller for first harmonic operation using a tridimensional, five to one scale model. The dimensions shown here correspond to the actual size in the cyclotron. The electrodes are shown as shaded areas. The dotted line indicates the orbit of the central ray particle described in Fig. 3.

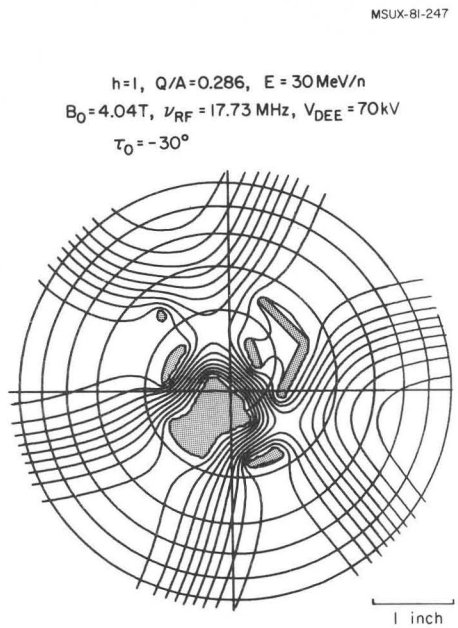

Fig. 3. Central region for h=1 (530 turns). The ion source and electrodes penetrating the median plane are shown as shaded areas. The equipotentials shown here correspond to all three dees having the same voltage and clearly indicate the outline of the six gaps. Note that for first harmonic operation, the three dees have voltages which are 120 deg out of phase. Thus, the static potential shown here is not the actual one, but only a simple superposition which is useful for outlining the electrodes and gaps. Superimposed on the equipotentials is the orbit for the central ray of the beam ($^{14}N^{4+}$) having the given parameters. This orbit emerges with a centering error of about 40 mils. This ion spends only five turns in the region covered by the measured potentials. The parameter τ_o is the starting time (in rf degrees) of the ion relative to the peak voltage between ion source and puller.

come close together in the machine center, and a careful study is required to determine their exact configuration.

For a given electrode geometry, the potential map $U_j(x,y)$ is measured with dee #j at full voltage, and with the other two dees both grounded. The three potential maps are then combined in the program to obtain the required time dependent potential: $V(x,y,t) = \sum_j U_j(x,y)\sin(\omega_{rf} t - k_j)$ where the sum covers j=1,2,3, and where $k_j = (j-1)2\pi h/3$ specifies the voltage phase of dee #j for operation on harmonic h. (The puller is attached to dee #1.)

Two examples of electrode geometries are shown in fig. 3 and fig. 4, along with the equipotential contours obtained from the measured potentials. Fig. 5 then shows the resultant time dependent potential V(x,y,t) obtained for the geometry in fig. 4 at three different t values.

The orbit computations in Part II of the program use θ as the independent variable so that r, p_r, z, p_z, t, and E are all dependent variables. For median plane motion, the potential and electric field are calculated as needed by combined interpolation and numerical differentiation of V(x,y,t).

The program treats only linear z motion and assumes for the vertical electric field:

$$E_z = z\left[(\partial^2 V/\partial x^2) + (\partial^2 V/\partial y^2)\right],$$

which follows from div $\vec{E}$=0. This assumption breaks down at electrode surfaces, and the program is equipped to detect these surfaces and to take suitable countermeasures.

For r > 2.8 in., the orbits enter Part III of the program which is almost identical to the spiral gap program described in detail in [3]. Here, the electric field is represented by a delta function for each of the six gap crossings occurring on each turn. However, the energy gain is modified by a transit time correction factor which takes account of the finite width of the electric gaps. In addition, when z motion is being calculated, the program provides a vertical impulse at each gap crossing in accordance with theoretical formulas given in [4].

This simple representation of the electric field effects allows Part III of the program to run very fast compared with the first two parts. Using a table of stored equilibrium orbit data, the program prints out once per sector the displacement of the accelerated orbit, thereby determining the centering error for this orbit.

Instead of ω_{rf}t, Parts II and III of the program use the "local" phase $\phi(\theta)$ for input and output, where this phase is defined in [3]. This $\phi(\theta)$ exhibits the effects of the radial oscillations and the orbit scalloping, as shown, for example, in fig. 6.

Part III of the program can run backward as well as forward, and backward runs starting from centered orbits provide valuable information for making a preliminary electrode design, which can then be used to obtain electrolytic tank measurements. These measurements, together with 3D-Cyclone orbit computations,

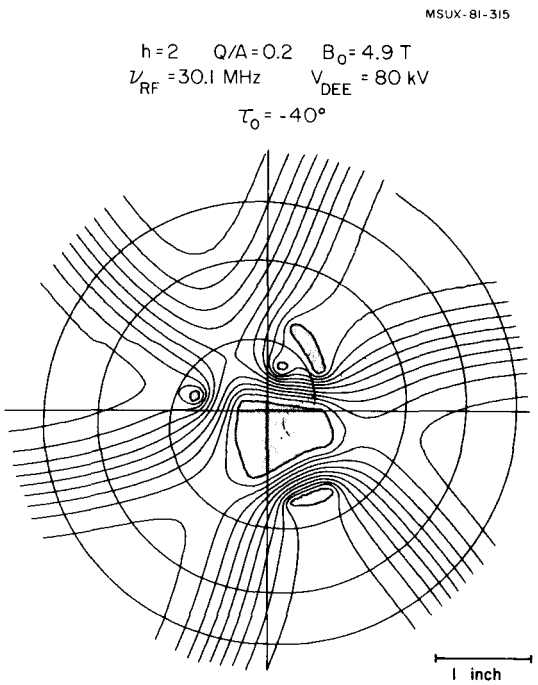

Fig. 4: Central region for h=2 (260 turns). The same as Fig. 3 but for second harmonic operation with a final total of 260 turns for the given ion. The central ray of the beam shown here finally emerges with a centering error of only a few mils. Because of the increase in transit time from source to puller compared to the h=1 case, source to puller separation is decreased to 0.8 cm from the 1.0 cm used for h=1. The maximum voltage will be decreased proportionately so as to maintain the same peak electric field. Note that the electrodes and ion source are substantially different from those used for first harmonic. When changing modes of operation, the tips of the dees will be removed or inserted through a vacuum lock mechanism.

will then either confirm the design or else indicate necessary revisions. This iteration process thus determines the final optimized design for a set of electrode structures.

Since the z motion is completely linear, the general solution, and hence the transfer matrix, can be generated from any two independent solutions like those shown, for example, in fig. 7. An auxiliary program has been developed which evaluates this transfer matrix as a function of θ, and then uses it to determine the maximum vertical acceptance (area of phase space ellipse) for a given central ray orbit. For a group of orbits whose initial (z,p_z) values completely cover this ellipse, the program then finds the vertical envelope (maximum value of z) as a function of θ, and this envelope (an example of which is also shown in fig. 7) reveals quite clearly the quality of the vertical focusing at different places in the central region.

Discussion of the results pertaining to the radial phase space behavior will not be presented here for lack of space.

*Supported by National Science Foundation Grant No. PHY80-17605.

[a]Present address: Institute of Nuclear Research, Shangai, People's Republic of China.
[b]Present address: Dept. of Physics, Jyväskylä, Finland.

[1]E. Liukkonen, J. Bishop, S. Motzny and T. Antaya, IEEE Trans. Nucl. Sci. NS-26 (1979) 2107.
[2]H.G. Blosser, 5th Int. Cyclotron Conf., (Butterworths, London, 1971), p. 257.
[3]M.M. Gordon, Nucl. Instrum. Methods 169 (1980) 327.
[4]M.M. Gordon and F. Marti, Particle Accelerators 11 (1981) 161.

MSUX-81-275

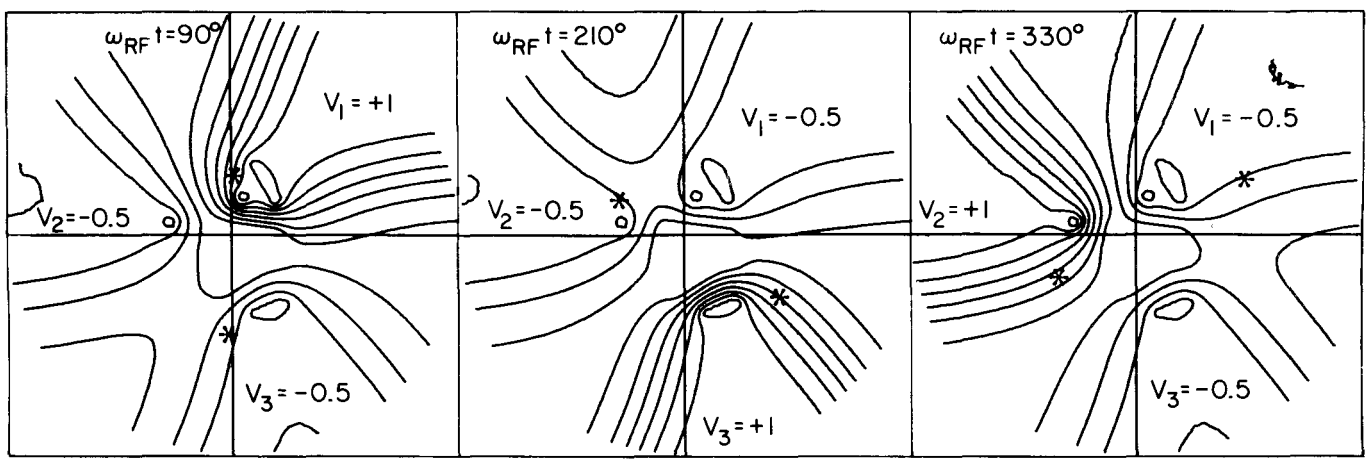

Fig. 5: Equipotentials for the h=2 central region at three different times. This figure shows the actual time dependent potential distribution for the h=2 electrode configuration of Fig. 4 as it would appear at three different t values. the asterisks indicate the simultaneous positions of the ions in the central ray orbit of Fig. 4. For h=2, there are two ion bunches per turn. Note that the electric field in the gap is higher when the ions exit the dees than when they enter. This indicates that the ions are injected with a positive phase (i.e. "late"), which is done purposely in order to increase the vertical electric focusing.

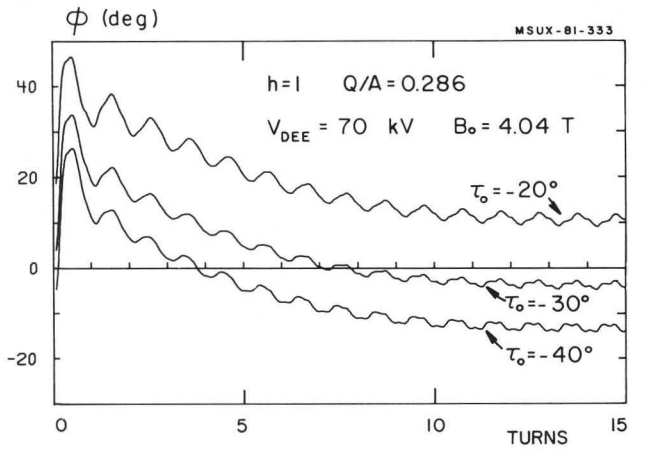

Fig. 6: Local phase for h=1 (530 turns) orbits. Evolution of the local phase for three ions starting 10 rf degrees apart from the source. Observe the 30 deg phase swing produced by the central magnetic cone. These curves show the once per turn oscillations ($\nu_r \approx 1$) characteristic of off-center orbits. (These orbits finally emerge with center displacements of 70, 40 and 60 mils reading from top to bottom.) In addition, a thrice per turn oscillation can be observed starting at about eight turns as a result of the three sector orbit scalloping. When these ions reach turn n=15, the average radius is about 4.5 inch.

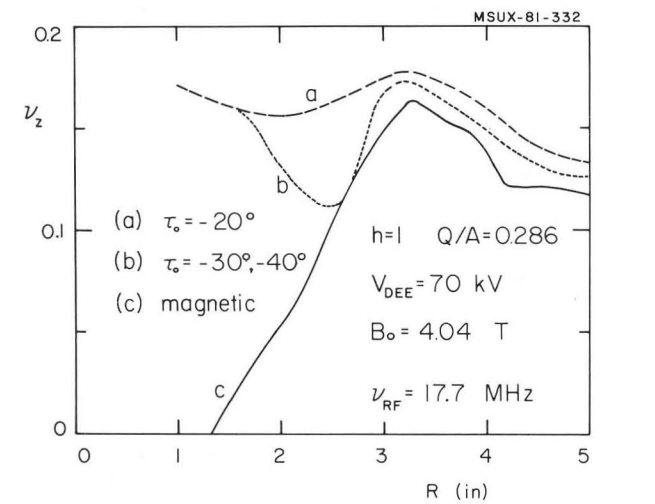

Fig. 8: Vertical focusing frequency versus radius for h=1 (530 turns) orbits. This figure presents estimates of ν_z vs. r derived from graphs similar to those at top and center of Fig. 7 for the three h=1 orbits whose phase variations are shown in Fig. 6. The solid curve gives the magnetic focusing values obtained from the equilibrium orbit code. Note the substantial improvement in ν_z produced by electric focusing at the lowest r values.

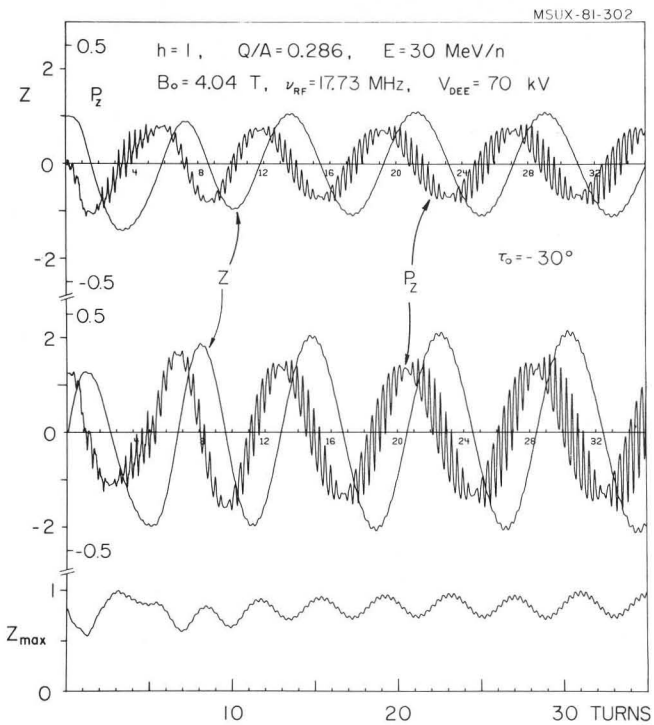

Fig. 7: Vertical motion and resultant beam envelope: The top and center curves show the z and p_z variations for two independent solutions representing the vertical motion for the h=1 central ray orbit shown in Fig. 3 and Fig. 6 (middle curves). Electric focusing dominates on the first few turns, and its importance relative to magnetic focusing declines steadily thereafter. As can be seen, the overall period of the vertical oscillations varies from about seven to nine turns, and superimposed on this variation is the thrice per turn oscillation due first to the gap crossings, and later to the magnet sectors. The bottom curve shows the corresponding variation of the beam envelope (normalized to a maximum of 1.0) which would be obtained for a beam matching the maximum vertical acceptance.